A modelling study for the integration of a PEMFC micro-CHP in domestic building services design

Alexandros Adam[a], Eric S. Fraga[a,*], Dan J.L. Brett[b]

[a] Centre for Process Systems Engineering, Department of Chemical Engineering, UCL, London WC1E 7JE, UK
[b] Electrochemical Innovation Lab, Department of Chemical Engineering, UCL, London WC1E 7JE, UK

HIGHLIGHTS

- MINLP optimisation model for the design of PEMFC fuel cell micro-CHP systems in dwellings.
- Process systems design approach considering fuel cell process units with dwelling's multiple heat demands.
- Heat emitter temperature constraints affects the optimum design and operation of the fuel cell micro-CHP system.

ARTICLE INFO

ABSTRACT

Fuel cell based micro-combined heat and power (CHP) units used for domestic applications can provide significant cost and environmental benefits for end users and contribute to the UK's 2050 emissions target by reducing primary energy consumption in dwellings. Lately there has been increased interest in the development of systematic methods for the design of such systems and their smoother integration with domestic building services. Several models in the literature, whether they use a simulation or an optimisation approach, ignore the dwelling side of the system and optimise the efficiency or delivered power of the unit. However the design of the building services is linked to the choice of heating plant and its characteristics. Adding the dwelling's energy demand and temperature constraints in a model can produce more general results that can optimise the whole system, not only the micro-CHP unit. The fuel cell has various heat streams that can be harvested to satisfy heat demand in a dwelling and the design can vary depending on the proportion of heat needed from each heat stream to serve the energy demand. A mixed integer non-linear programming model (MINLP) that can handle multiple heat sources and demands is presented in this paper. The methodology utilises a process systems engineering approach. The model can provide a design that integrates the temperature and water flow constraints of a dwelling's heating system with the heat streams within the fuel cell processes while optimising total CO_2 emissions. The model is demonstrated through different case studies that attempt to capture the variability of the housing stock. The predicted CO_2 emissions reduction compared to a conventionally designed building vary from 27% to 30% and the optimum capacity of the fuel cell ranges between 1.9 kW and 3.6 kW. This research represents a significant step towards an integrated fuel cell micro-CHP and dwelling design.

1. Introduction

Energy and environment are becoming key matters in the modern world. Climate change, instability in energy supply and the desire for national self-sufficiency are all energy related concerns at the top of political agendas worldwide. As world's population is increasing, cities are growing larger and energy demand is rising. The International Energy Outlook 2015 projects that world energy consumption will grow by 28% between 2017 and 2040, a demand primarily driven by developing countries [1]. As fossil fuels resources are depleting and nuclear power imposes a safety risk, a sustainable way of producing energy is required to ensure that the predicted increase in energy consumption can be satisfied.

The amount of energy that is consumed by all buildings, commercial and domestic, is responsible for about 45% of total energy consumption in the UK and contributes significantly to climate change [2]. New energy efficient technologies for micro-generation have been implemented that can reduce CO_2 emissions and fulfil the energy demand in buildings. Renewable technologies that have been used in buildings include photovoltaic cells, solar thermal panels, wind turbines, ground

source heat pumps, biomass and others. A technology that is suitable for dwelling applications and has seen significant development in the recent years is Combined Heat and Power.

Combined Heat and Power (CHP) or otherwise called cogeneration is the use of one process to simultaneously generate both electricity and useful heat. Cogeneration is a technique that allows primary energy savings as the production of electricity (from power plants) and heat (from boilers) is separate. There are various technologies that can be used as the driving force of a CHP system and their suitability depends on the scale of the application, the energy characteristics and the economics.

Energy demand in domestic dwellings is largely provided by conventional means, grid electricity and gas fired boilers. However, micro-CHP systems powered by fuel cells could be used to serve domestic loads efficiently, meet heating and some electricity needs of residential dwellings. This technology can achieve higher electrical efficiencies than heat engines and has the potential to reduce carbon dioxide emissions in the domestic sector. It can be an alternative way of meeting residential energy needs if capital cost targets can be met [3].

The design of fuel cell based micro-CHP systems is a complex task as all components need to be sized appropriately to satisfy the domestic energy demand profile and to serve heat loads effectively. Overestimating or underestimating the size of a CHP unit decreases its potential. Residential electricity, heating and hot water demands fluctuate daily and seasonally. Similarly the operation of the fuel cell micro-CHP is subject to constraints. It is therefore important to define the operation strategy (scheduling of demands, electricity/heat generation, etc.) and the control method that is utilised to meet the building energy demands because they define the overall performance and efficiency of the building energy system as a whole.

This paper presents a MINLP model for an domestic building services design using a fuel cell based micro-CHP system. It is systematic design tool that can improve the design of fuel cell micro-CHPs in dwellings by providing better understanding of the temperature constraints in the plant-dwelling system. Four case studies are presented in this paper examining different scenarios.

2. Background

Many authors have developed models to predict how fuel cell micro-CHP systems would perform in a domestic environment. The use of models to examine various scenarios is mainly due to the fuel cell micro-CHP being an emerging technology with small market share. Common goals include the estimation of the environmental benefits in terms of CO_2 emissions reductions and primary energy savings, or the reduction in operating costs from reduced purchase of electricity. Researchers choose simulation or optimisation methods in order to calculate values for their chosen design variables. The various models in literature vary in terms of level of detail and system boundary. [4].

Optimisation can provide useful results as the fuel cell micro-CHPs and their design is currently under development, so optimisation techniques can identify ways of improving it. Many studies based on single objective optimisation have chosen total cost as the design

objective. Staffell et al. estimated the cost target for a 1 kWe fuel cell at £280–500 per kW in order to compare with boiler technologies [5]. This is far from the current range of costs and until high production rates can be reached, such low prices are difficult to be achieved. A study that investigated the requirements for high market penetration of various micro-CHP technologies concluded that low capital and fuel cost prices would allow micro-CHPs with low heat-to-power ratio, such as fuel cell based units, to increase their market share [6]. A possible way for this is by government incentives and change in policy [7].

Techno-economic studies usually apply multi-objective optimisation methods and identify trade-offs between cost and a technical characteristic such as electrical efficiency or delivered power [8]. A techno-economic study was performed by Hawkes et al. in a two-part report that calculated the maximum additional capital cost an investor would pay for the fuel cell micro-CHP system over and above what they would pay for a competing conventional heating system and the impact of stack degradation on economic and environmental performance [3,9]. Arsalis et al. model a high temperature PEMFC based micro-CHP for residential applications in a Danish household maximising efficiency using a 1 kWe and 2 kWth unit [10,11]. Ashari et al. performed an exergy, economic and environmental analysis of a PEMFC micro-CHP for a household in Tehran. They concluded that should the fuel cell micro-CHP provided the entire electricity and thermal demand a nominal capacity of 8.5 kWe is needed [12]. Barelli et al. performed a dynamic analysis of a PEMFC aiming to evaluate system performance and efficiency under the variable loads of households [13]. Dorer et al. performed an assessment of fuel cell micro-CHP systems (PEMFC and SOFC) for different building types[14]. They calculated efficiency and CO_2 emissions and analysed fuel cell sizing in relation to residential heating demand. The concluded that a robust assessment of fuel cell systems for micro-CHP applications requires a refined methodology that considers dynamic conditions. Gigliucci et al. developed a mathematical model to predict the performance and operating parameters under off-design conditions of a prototype fuel cell based micro-CHP unit installed in a site in Italy [15].A multi-objective optimisation study was performed by Ang et al. that calculated the trade-offs between power output and fuel consumption of a fuel cell based micro-CHP in heat-led operation [16]. The influence of the geographic location in the performance of micro-CHP systems has been examined by Mago and Luch [17] and the results demonstrate the importance of the power to heat demand of a dwelling in the performance of the micro-CHP system. A study that moves one step forward in terms of the involvement of the dwelling side of the fuel cell micro-CHP system was conducted by Gandiglio et al. [18]. They have modelled a 1 kWe Proton Exchange Membrane Fuel Cell (PEMFC) based micro-CHP system together with the balance of plant (all auxiliary components required for the fuel cell system to operate reliably), coupled with a constant temperature underfloor heating system. However, even though the heating system is considered, no system sizing is attempted as the study is based on the fixed choice of a 1 kWe fuel cell unit.

Particular attention has been given recently in modelling thermal storage tanks (TST) when used with micro-CHP systems. The common point of most publications is that they identify the optimum size of the storage tank among different criteria. The constraints vary and could be the total cost, space limitations or profit (when export tariffs are included). Publications that focus on the effect of thermal storage are included in references [19–21].

In most studies the focus is primarily on identifying design parameters within the fuel cell CHP boundary itself that minimise cost or energy but there is limited information on heat integration between the fuel cell and the building services design. The design of the heating system that the fuel cell micro-CHP would be plugged into is not considered in most models. The water mass flow rates and temperatures in the heating and domestic hot water (DHW) pipework determine this design. This design involves understanding of low temperature hot water (LTHW) systems and imposes limitations on sizing, control and

operation of the selected plant. The influence of components ranging from the balance of plant to the pipe network could be considered in designing and optimising a fuel cell micro-CHP system for residential applications. The main challenge in process design lies in identifying how the various processes are interlinked to affect the heat quality and amount of energy production [22]. There is a link between the type of fuel cell chosen in the design, its heat output and how it can be efficiently applied into a dwelling's heat distribution system.

3. Problem description

In this paper the design of the a fuel cell micro-CHP system coupled with all its supportive systems such as a gas boiler and a TST in a grid-connected dwelling is considered. PEMFCs set up for micro-generation deliver heat at the exit of the afterburner and at the cooling circuit of the cell. Each heat stream can be utilised to supply heat to space heating, DHW or supply heat to a TST. In the design of fuel cell micro-CHPs systems in dwellings the exact sizing and connections between all components of the design has to be determined. The ways these components are connected define how the energy demand is met. Residential electricity, heating and hot water demands vary continuously with daily and seasonal cycles. The plant involved in a dwelling design using fuel cell micro-CHP has variability in temperature and heating water flow rates. As heating sources and demands exist at different temperatures and profiles, a design that considers this variability and can bring them together is achievable. Fig. 1 shows the various heat streams that can be harvested from a fuel cell, gas boiler and thermal storage including the ways in which they can be integrated

into the building heating services.

3.1. Modelling methodology

The purpose of the model is to identify optimal connections between power and heat generation plant with the energy demand side of the dwelling while minimising CO_2 emissions. The model considers possible interconnections between plant and demand, together with system sizing. The basic principles of the model are listed below:

- The fuel cell generates electricity and heat, consuming H_2 reformed from natural gas in the external reformer.
- The heat required for reforming is recovered from the afterburner stream.
- Heat for use in the dwelling is recovered by the fuel cell stack cooling circuit and at the afterburner exhaust stream.
- A natural gas boiler supplements the heat recovered by the fuel cell stack and the afterburner to satisfy heat demand of the dwelling.
- The electricity grid supplements the electricity generated by the fuel cell to satisfy the power demand of the dwelling.
- All heat recovered from the fuel cell processes and generated by the boiler can be used in separate space heating and domestic hot water circuits via a low temperature hot water circuit.
- A thermal storage tank can store heat from either fuel cell heat sources.
- There are two low loss headers used to separate primary (source) and secondary (demand) circuits. Pipework connected to one header is used to supply heat to the space heating circuit, while the
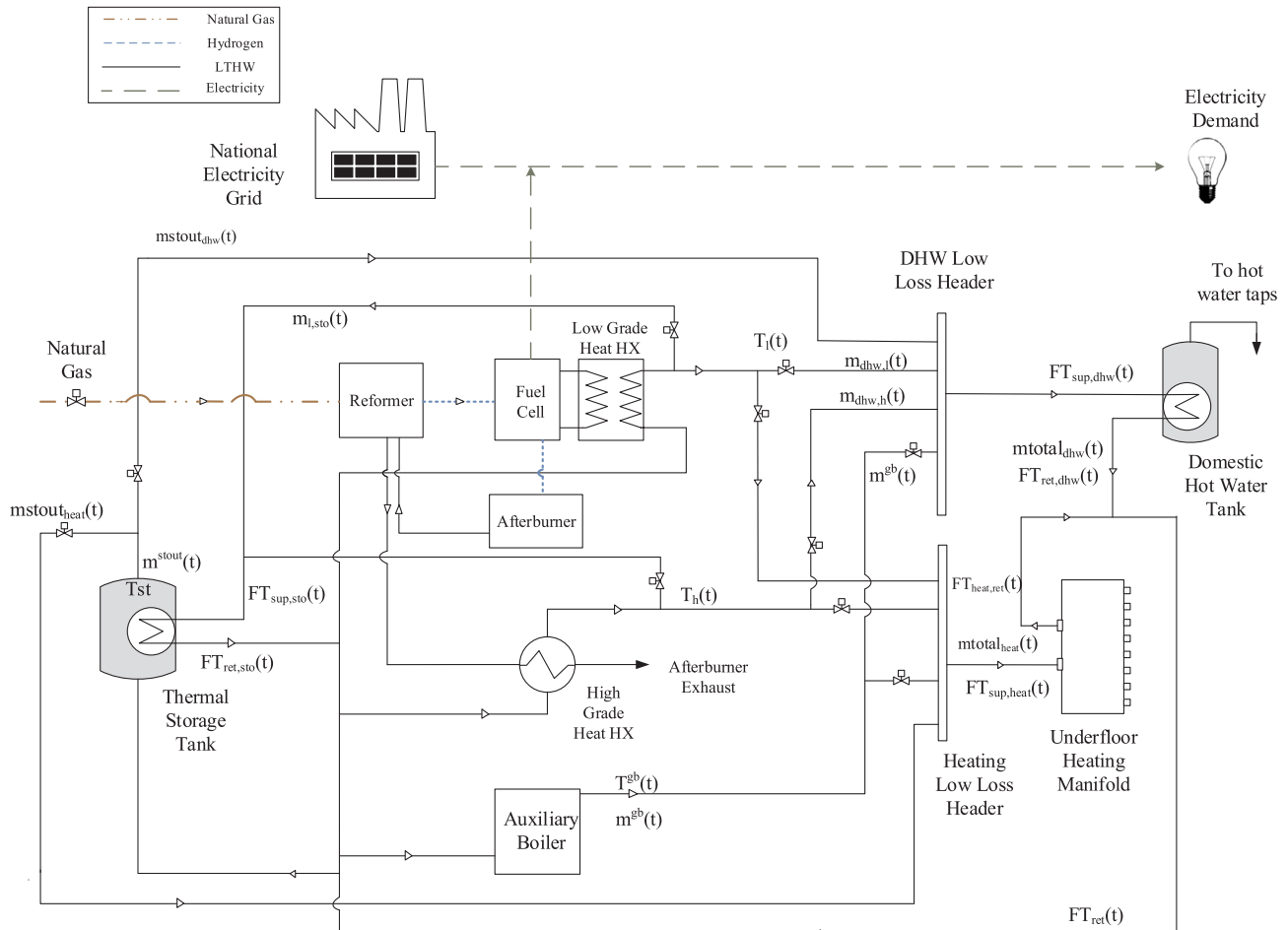

Fig. 1. PEMFC based micro-CHP model schematic diagram demonstrating the various sub-components and pipework connections included in the design. Some the variables used by the model are shown as labels.

Table 1
Description of the mathematical symbols used in the model.

Indices		
s (CH₄, H₂, CO₂)	Species	–
t (1,…,288)	Timestep	–
g (h,l)	FC Heat Exchanger (FC Cooling Circuit or Afterburner)	–
j (Heat,dhw,sto,ele)	Type of Energy Demand	–
p (sup,ret)	Supply or Return position on pipework	–
Parameters		
$Q_j^{req}(t)$	Dwelling Energy Demand	kW
T^{env}	Environment Reference Temperature	°C
E^{th}	Theoretical fuel cell voltage	V
ra	Fuel cell ramp up	kW/s
q^{ref}	Heat required for the reforming process	kJ/mol
i_{H2}	Electrical current of fuel cell from hydrogen flow	kAsec/mol
MW^s	Molecular Weight of species s	kg/mol
HHV^s	Higher Heating Value of species s	kJ/mol
cp	Specific Heat Capacity of Water	kJ/kgK
f_e	Emissions factor for electricity grid	kg/kWh
n^{gb}	Boiler Efficiency	–
n^{hx}	Heat Exchanger Efficiency	–
A_j^{gb}	Boiler Maximum Heat Output per demand j	kW
A_{gj}^{fc}	Fuel cell Maximum Heat Output per demand j per heat exchanger g	kW
B_j^{st}	Temperature constraint for demand j	°C
δt	Timestep	sec
Variables		
$n_s^{fc}(t)$	Molar Flow Rate of species s in fuel cell at time t	mol/s
$m_s^{fc}(t)$	Mass Flow Rate of species s in fuel cell at time t	mol/s
$n_s^{gb}(t)$	Molar Flow rate of species s in gas boiler at time t	mol/s
$m_s^{gb}(t)$	Mass Flow rate of species s in gas boiler at time t	mol/s
V^{st}	Storage Tank Volume	m³
$V^c(t)$	Fuel cell Voltage at time t	V
$U^{fc}(t)$	Hydrogen Utilisation at time t Factor	–
$FT_{p,j}(t)$	System Temperature at flow p, demand j at time t	°C
$T^{gb}(t)$	Boiler Temperature at time t	°C
$T_g(t)$	Heat Exchanger Temperature at grade g at time t	°C
$T^{st}(t)$	TST Temperature at time t	°C
$E^g(t)$	Grid Electricity	kW
$E^{fc}(t)$	Fuel Cell Electrical Output at time t	kW
$E^{exp}(t)$	Exported Electricity to the grid at time t	kW
$Q_j^{gb}(t)$	Boiler Output at time t and demand j	kW
$r^{gb}(t)$	Load factor of Gas Boiler	–
Pgb	Maximum capacity of Gas Boiler	kW
$Q_{g,j}(t)$	Fuel cell heat output of g heat exchanger at time t and demand j	kW
$E^{st}(t)$	Heat stored in TST	kJ
$Q_j^{stout}(t)$	TST Heat Output at time t and demand j	kW
$Q^{bur}(t)$	Heat generated from hydrogen combustion at time t	kW
$Q^{ref}(t)$	Heat required for reforming at time t	kW
$m_j^{total}(t)$	Total System Water Flow rate at time t and demand j	kg/s
$m_j^{stout}(t)$	TST Water Flow rate at time t and demand j	kg/s
$m_j^{gb}(t)$	Boiler Flow rate at time t and demand j	kg/s
$m_{gj}(t)$	Flow rate at fuel cell grade g at time t and demand j	kg/s
M^{fc}	CO₂ emissions caused by fuel cell	kg
M^{gb}	CO₂ emissions caused by gas boiler	kg
M^{el}	CO₂ emissions caused by grid electricity	kg
M^{exp}	CO₂ emissions savings by exporting electricity to the grid	kg
z	Total CO₂ emissions	kg

Table 1 (*continued*)

Binary variables		
$y_j^s(t)$	1 if temperature constraint is activated for demand j, 0 otherwise	–
$y_{gj}(t)$	1 if fuel cell heat source g releases heat to demand j, 0 otherwise	–
$y_j^{gb}(t)$	1 if gas boiler releases heat to demand j, 0 otherwise	–
$y_j^{stout}(t)$	1 if TST releases heat to demand j, 0 otherwise	–

domestic hot water tank is served from a different header.

3.2. Mathematical formulation

Table 1 lists the mathematical symbols used in the model.

The overall problem is formulated as MINLP model. Binary variables are used to introduce links between variables. The yearly analysis is made on a dataset that consists of 288 hourly timesteps of energy demands. A month, therefore is represented by a single day or 24 timesteps. This dataset is detailed enough and can capture the variation of dwelling energy demand that occurs during the year but at the same time is small enough to allow for flexibility in the modelling process.

3.2.1. Fuel cell stack

The central part of the system is the fuel cell stack. Fig. 2 shows a labelled diagram of the fuel cell showing incoming and outgoing flows.

The fuel cell electricity production $E^{fc}(t)$ as a function of the hydrogen flow rate $n_{H2}^{fc}(t)$, the fuel utilisation factor $U^{fc}(t)$, the electrical current produced by each mol of hydrogen i_{H2} [23] and the operating cell voltage $V^c(t)$, can be given by the following equation:

$$E^{fc}(t) = n_{H2}^{fc}(t) \cdot U^{fc}(t) i_{H2} \cdot V^c(t) \tag{1}$$

The amount of heat that is generated depends on the difference between the open circuit voltage E_{th} and the operating value.

$$P_{th}(t) = n_{H2}^{fc}(t) \cdot i_{H2} \cdot (E^{th} - V^c(t)) \tag{2}$$

Not all heat can be recovered by the cooling medium, so a heat exchanger recovery efficiency determines the recoverable heat from the fuel cell. The cooling water circuit of the fuel cell prevents stack overheating and protects the membrane from drying. The cooling water exits the fuel cell stack at a temperature between 60 and 80 °C. The return temperature of the cooling water to the fuel cell stack has a 5–20 °C temperature difference to the water exit temperature from the fuel cell stack [15].

$$Q_l^{fc}(t) = \eta_{hx} \cdot n_{H2}^{fc}(t) \cdot i_{H2} \cdot (E^{th} - V^c(t)) \tag{3}$$

where the subscript "l" refers to the low grade heat delivered from the cooling circuit of the fuel cell.
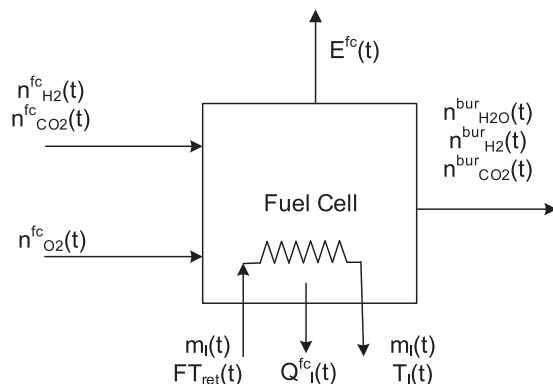
Fig. 2. Schematic of the fuel cell stack showing mass and energy flows.

Heat from the cooling circuit heat exchanger $Q_l^{fc}(t)$ to the dwelling satisfies Eq. (4). The total heat from the cooling circuit is the sum of heat delivered to all demands j.

$$Q_l^{fc}(t) = \sum_j Q_{l,j}(t) = \sum_j m_{l,j}(t) cp(T_l(t) - FT^{ret}(t)) \tag{4}$$

3.2.2. Reformer

The following reaction takes place at the reformer and produces the hydrogen that is consumed by the fuel cell.

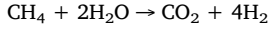$CH_4 + 2H_2O \rightarrow CO_2 + 4H_2$

Fig. 3 shows a labelled diagram of the reformer showing incoming and outgoing flows.

Mass balances performed at the reformer deliver the quantities of the resulting H_2 and CO_2 :

$$n_{CO2}^{fc}(t) = n_{CH4}^{fc}(t) \tag{5}$$

$$n_{CH4}^{fc}(t) = \frac{n_{H2}^{fc}(t)}{4} \tag{6}$$

$$m_s^{fc}(t) = MW_s \cdot n_s^{fc}(t) \tag{7}$$

where $n_s^{fc}(t)$ represents the molar flow rate at time t of species s in the fuel cell, $m_s^{fc}(t)$ the mass flow rate and MW_s the molar weight. "s" denotes species CH_4, H_2, CO_2 involved in the system.

3.2.3. Afterburner

Hydrogen that is not used in the fuel cell is combusted in the afterburner. Fig. 4 shows a labelled diagram of the afterburner showing incoming and outgoing flows.

The amount of heat generated by combustion of hydrogen is a function of the hydrogen flow rate in the afterburner $n_{H2}^{bur}(t)$ and the calorific value of the fuel HHV_{H2}.

$$Q^{bur}(t) = n_{H2}^{bur}(t) \cdot HHV_{H2} \tag{8}$$

The molar flow to the afterburner is equal to the fuel that is not used in the fuel cell:

$$n_{H2}^{bur}(t) = (1 - U^{fc}(t)) n_{H2}^{fc}(t) \tag{9}$$

The hydrogen utilisation factor is defined as the ratio between the hydrogen flow rate that reacts in the stack and the hydrogen flow input to the stack and in the model it has been constrained between 0.6 and 0.85 according to usual design specifications of PEMFCs [24]. Although almost 100% utilisation of hydrogen can be achieved with dry feeds of hydrogen and oxygen [25], this would require finding an alternative source for providing reforming heat such as burning natural gas.

The exhaust gases leave the combustion chamber at 700–800 °C and provide heat for the reforming process which requires high temperatures to occur [26]. The heat required for reforming is a function of methane flow rate $n_{CH4}^{fc}(t)$ and the energy that is required to reform one mole of CH_4 to H_2 [26].

$$Q^{ref}(t) = n_{CH4}^{fc}(t) \cdot q^{ref} \tag{10}$$

Useful heat $Q_h^{fc}(t)$ can be recovered from the exhaust gases after they have released heat for the reforming process at 400 °C [26]. The gases enter a heat exchanger where heat can be recovered and used in the dwelling.

$$Q_h^{fc}(t) = Q^{bur}(t) - Q^{ref}(t) \tag{11}$$

The remaining heat is recovered by a heat exchanger and it can be used for space heating, DHW or stored in the TST (all demands are represented by index $j \in \mathcal{J}$). This heat is modelled using Eq. (12).

$$Q_h^{fc}(t) = \sum_j Q_{h,j}(t) = \sum_j m_{h,j}(t) cp(T_h(t) - FT^{ret}(t)) \tag{12}$$

At times when $Q^{bur}(t) = Q^{ref}(t)$ there is no remaining heat from the afterburner to be used in the building as all is used for reforming.

3.2.4. Gas boiler

At the boiler, natural gas is combusted to produce H_2O and CO_2 based on the methane combustion reaction. In this case it has been assumed that natural gas is pure methane

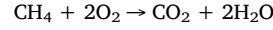$CH_4 + 2O_2 \rightarrow CO_2 + 2H_2O$

Fig. 5 is a labelled diagram of the gas boiler showing incoming and outgoing flows.

Mass balance is then performed in a similar way at the gas boiler resulting at the following equations

$$n_{CO2}^{gb}(t) = n_{CH4}^{gb}(t) \tag{13}$$

$$m_s^{gb}(t) = MW_s n_s^{gb}(t) \tag{14}$$

where $n_s^{gb}(t)$ represents the molar flow rate at time t of species s in the gas boiler and $m_s^{gb}(t)$ the mass flow rate.

Boiler heat $Q_j^{gb}(t)$ to demand j is given by Eq. (15), where $T^{gb}(t)$ is the boiler supply temperature, cp is the specific heat capacity of water.

$$Q_j^{gb}(t) = m_j^{gb}(t) \cdot cp \cdot (T^{gb}(t) - FT^{ret}(t)) \tag{15}$$

Boiler heat is also has to satisfy Eq. (16).

$$\sum_j Q_j^{gb}(t) = n_{CH4}^{gb}(t) \cdot HHV_{CH4} \cdot \eta^{gb} \tag{16}$$

where η_{gb} represents the efficiency of the boiler.

Also,

$$\sum_j Q_j^{gb}(t) = r^{gb}(t) P^{gb} \tag{17}$$

where $r^{gb}(t)$ represents the load factor and P^{gb} the maximum capacity of the gas boiler.

3.2.5. Thermal storage tank

The energy content of the storage tank E^{st} (kJ) is given by Eq. (18).

$$E^{st}(t) = V^{st} \cdot \rho \cdot cp \cdot (T^{st}(t) - T^{emv}(t)) \tag{18}$$

where V^{st} (m³) is the storage volume, ρ the water density and $T^{env}(t)$ (°C) a reference environmental temperature.

Energy balance in the storage tank is given by Eq. (19).

$$\frac{d}{dt} E^{st}(t) = \sum_g Q_{g,sto}(t) - \sum_j Q_j^{stout}(t) \tag{19}$$

As there is no heat flow from the TST to the TST, for j = sto, $Q_{sto}^{stout}(t) = 0$.

Temperature constraints have been introduced in the TST model. There is a temperature limit below which the storage tank cannot release heat to the dwelling. A constraint of 40 °C for underfloor heating
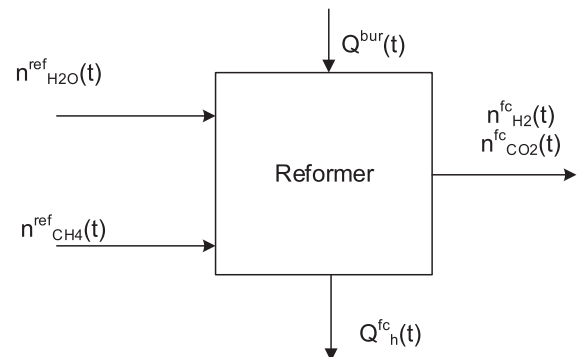

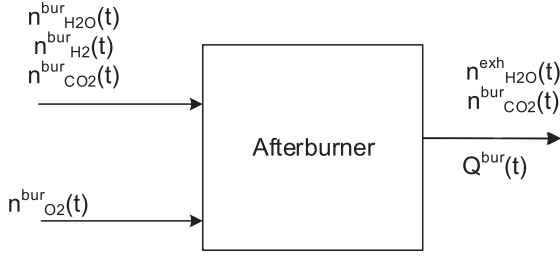Fig. 3. Schematic of the reformer showing mass and energy flows.

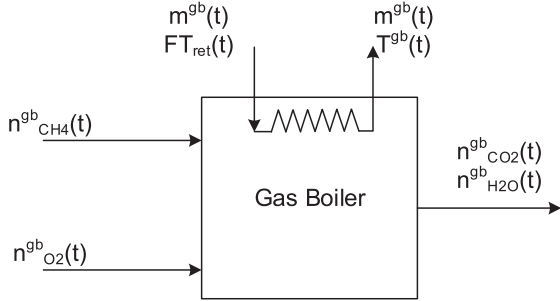**Fig. 4.** Schematic of the afterburner showing mass and energy flows.

Fig. 5. Natural Gas Boiler Schematic showing mass and energy flows.

(UFH) and 60 °C for radiators has been used in the model before heat can be used for space heating. The constraint is 60 °C for DHW. This is to ensure that water flow from the storage is of sufficient temperature to be used in the pipe circuit that serves the associated heat emitting system.

This constraint was modelled using binary variable $ys_j(t)$ which is linked to both T_{st} and Q^{stout} as shown in Eqs. (20) and (21). δt is the relevant time period. In this case as the analysis is performed in hourly timesteps, δt is 3600 s.

$$Q_j^{stout}(t) \leqslant E^{st}(t)\frac{ys_j(t)}{\delta t} \tag{20}$$

$$T_j^{st}(t) \geqslant B_j^{st}\,ys_j(t) \tag{21}$$

for $T_j^{st}(t), Q_j^{stout}(t) \geqslant 0$.

Discharge heat $Q_j^{stout}(t)$ to demand j is given by Eq. (22), where $m_j^{stout}(t)$ is theTST water flow rate at time t and demand j

$$Q_j^{stout}(t) = \sum_j m_j^{stout}(t)\cdot cp\cdot(T^{st}(t) - FT^{ret}(t)) \tag{22}$$

3.2.6. Pipe network and heat emitters

Water flows are mixed in the two low loss headers as shown on Fig. 1.

Water mass balances are performed in the pipework network where different flows come together, i.e.

$$m_j^{total}(t) = m_{h,j}(t) + m_{l,j}(t) + m_j^{gb}(t) + m_j^{stout}(t) \tag{23}$$

Also, $m_j^{stout}(t) = m_j^{gb}(t) = 0$ for j = sto.

The water mass flow required for the space heating and DHW in order to maintain a 10 °C temperature difference in the demand side is calculated in each step using the following relation:

$$m_j^{total}(t) = \frac{Q_j^{req}(t)}{C_{pw}\cdot 10} \quad \text{for } j = HEAT, DHW \tag{24}$$

A modern variable flow water system has been assumed for the design, compared to a constant flow option, which varies in each timestep providing heat to the demand. In such a system an adjustment in energy output requires a water flow change.

Also,

$$Q_j^{req}(t) = Q_j^{gb}(t) + Q_j^{stout}(t) + \sum_g Q_{g,j}(t) \tag{25}$$

The term $\sum_g Q_{g,j}(t)$ represents the summation of the amount of heat delivered to demand j from the g fuel cell heat exchanger.

Heat emission from the heating and DHW system also needs to satisfy the following equation:

$$Q_j^{req} = m_j^{total}(t)\cdot cp\cdot(FT_{sup,j}(t) - FT_{ret,j}(t)) \tag{26}$$

Binary variables have been used in the model in definitions of upper and lower bounds of heat output variables. Indicatively

$$Q_j^{gb}(t) \leqslant y_j^{gb}(t)A_j^{gb} \tag{27}$$

where A_j^{gb} is the upper bound of the heat output of the boiler per demand j

Therefore the mass balance becomes:

$$m_j^{total}(t) = y^{gb}(t)m_j^{gb}(t) + y_j^{stout}(t)m_j^{stout}(t) + \sum_g (y_{g,j}(t)m_{g,j}(t)) \tag{28}$$

where $A_{g,j}^{fc}$ is the upper bound of the heat output of heat exchanger g to demand j.

3.2.7. Electricity energy balance

The electricity output of the fuel cell at time t $E^{fc}(t)$ and the electricity import from the grid at $E_g(t)$ time t have to be equal to the electricity demand $Q_{ele}^{req}(t)$ as shown in Eq. (22),

$$Q_{ele}^{req}(t) = E^{fc}(t) + E_g(t) \tag{29}$$

3.2.8. Total system CO$_2$ emissions

The objective function is to minimise the total system CO$_2$ emissions resulting from the operation of the fuel cell and gas boiler and the imported grid electricity. For the grid electricity, emissions rates for every unit imported of energy have been used, as described in [27]. Many studies have chosen cost as their objective function. According to Staffell et al. though "There is considerable uncertainty in the cost targets for fuel cell CHP" [5]. This uncertainty would be carried on the results of any modelling attempt based on cost. An objective function based on CO$_2$ emissions on the other hand, is free of this problem as it depends on plant efficiencies and energy balances. Therefore the choice of total CO$_2$ emissions as an objective function represents more accurately than cost, a model that attempts to design a system such as the one shown in Fig. 1. Nevertheless. the implemented model can also be used to minimise cost with small modifications, if accurate cost models become available.

$$M^{fc} = \sum_t m_{CO2}^{fc}(t) \tag{30}$$

$$M^{gb} = \sum_t m_{CO2}^{gb}(t) \tag{31}$$

$$M^{el} = f_e \sum_t E^g(t) \tag{32}$$

$$min\,z = M^{fc} + M^{el} + M^{gb} \tag{33}$$

3.3. Assumptions

A few simplifying assumptions are made in the fuel cell and gas boiler models:

- Natural gas used in the system is assumed to be pure CH$_4$.
- There is atmospheric pressure on the fuel cell processes. Even though PEMFCs can be operated at higher pressures, a possible drop in system efficiency could be caused by the energy needed for air compression.

- It has been assumed that all methane is converted to hydrogen, where in reality a 100% conversion at the reformer is not possible and some methane is present in the reformate.
- It has been assumed that all CO is fully converted to CO_2 in the water-gas shift reaction in the reformer. The unconverted carbon monoxide from the reformer can reduce the activity of the anode and lead to stack voltage reduction.
- It has been assumed that all heat of the afterburner exhaust stream exiting the reformer can be recovered.

These assumptions relate to the fuel and air inputs of plant and it is expected that they could only affect the amount of electricity and heat generation by a small percentage.

On the LTHW circuit the following assumptions were made:

- There are no heat losses or thermal stratification included in the TST model. This assumption is considered to have small effect on the model results because the datasets are small and the cumulative amount of thermal losses from the TST would not make a significant difference in the objective function or alter the results in terms of system sizing and operation.
- It is assumed that low loss headers are used in the design which means that multiple sources can connect to them.

The intention of the model is to identify optimal connections between subcomponents and to identify optimal capacities of plant. It is therefore considered that the above assumptions have small effect on the designs represented in the model.

4. Dwelling energy data

A base case has been developed according to existing literature sources and own interpretation. The base case building is modelled with building modelling software and is a house served by a conventional heating, DHW and electricity systems. It is located in London and is a four bedroom house with two storeys; a total floor area of about 190 m². The base case is a building which is compliant with Building Regulations Part L1A with regard to the U values and air permeability [28]. Table 2 shows the U values that have been used in this study for the base case building. The air permeability is set at $5\,\frac{m^3}{m^2\,h}$ at 50 Pa.

- Heating is provided by a gas fired condensing boiler. Boiler system efficiency for the base case is compliant with Domestic Heating Compliance Guide [29]. Boiler efficiency is set at 90%.
- Two heating systems are examined (UFH and radiators), therefore two base cases are established.
- Electricity is supplied from the grid.

Fig. 6 shows an image of the produced model.

The heating demand for two different heating systems has been identified to formulate two base cases. The two options are an UFH and a radiator system. The underfloor heating system being generally a slow response system requires longer heating hours and less peaks compared to a radiator system. The space heating demand for the base case building served by underfloor heating can be seen in Fig. 7.

A 24-h segment of the annual dataset presented in Fig. 7 can be extracted to show the daily variation of space heating demand such as the one shown in Fig. 8. The graph shows the daily variation of space heating demand of the UFH and radiator systems and demonstrates the differences of the heating pattern, which allows for longer heating periods without many peaks for the UFH system compared to radiators.

5. Analysis, results and discussion

Four case studies for fuel cell micro-CHP designs are evaluated in

terms of their CO_2 emissions and compared to the base case presented in chapter 4. In these case studies, the heat generating plant is a fuel cell and a gas fired boiler and the heat emitter is underfloor heating for cases 1 and 2 and radiators for cases 3 and 4. The effect of TST in the design and operation of the building is evaluated in cases 2 and 4 that include a TST connected to the fuel cell heat exchangers as shown in Fig. 1.

The model was implemented in GAMS [30] and was solved on an Intel Core i5-2500 CPU, 4 GB RAM, 3.3 GHz computer. The resulting optimisation model is non-linear and non-convex and was solved using the global optimisation solver ANTIGONE [31]. The model statistics of the implemented MINLP model can be seen in Table 3. The optimality gas was set to 1% for all cases presented in this study.

Table 4 summarises the reduction in CO_2 emissions for all case studies compared to the base case. The reductions in CO_2 emissions from the base case vary between 27% and 30%. The base case emissions are derived from the reference building.

Table 5 lists the resulting capacities for the gas boiler, fuel cell and TST volume.

Table 6 summarises the annual contribution of each heat source to space heating and DHW demand for all case studies.

5.1. Underfloor heating system

Heating in Case 1 is satisfied from the two heat sources of the fuel cell (the high grade heat of the afterburner and the lower grade heat of the cooling circuit) and the gas boiler. This is illustrated in Fig. 9 for the 288 h dataset. Winter is represented by timesteps 1–72, spring 73–144, summer 145–216 and autumn 217–288.

In case 2, heat from the cooling circuit and the afterburner of the fuel cell is used for heating, DHW and for charging the TST. The heat that they deliver to the dwelling on a winter day can be seen in Fig. 10 (for timesteps 1–24 of the 288 dataset). The graph demonstrates that the demand is covered by a combination of heat sources giving flexibility to the system by storing heat in the TST and allowing the fuel cell to cover the whole electricity demand.

The temperature of the storage tank has been assumed to be at 50 °C initially and was set be above 40 °C at the end. The optimum volume of the storage tank is 140 L. The upper bound was selected to be 800 L. However the low volume of the storage tank compared to its upper bound ensures that water above the 45 °C heating threshold would be more easily available in the TST. 800 l of water would require more fuel cell heat to be raised to 45 °C. Fig. 11 shows the variation of the TST temperature. It can be seen that at the end of each day the temperature is equal to the start of the day. In the figure it is also shown that the otherwise wasted summer heat is stored in the TST increasing water temperature. The temperature in the TST increases above 50 °C in the summer when heat from the fuel cell that is not needed in the system is stored in the TST.

Case 2 covers electricity by using the fuel cell with no electricity input from the grid compared to case 1 where a small amount of electricity is imported. The fuel cell in case 2 is allowed to operate for more hours and satisfy the entire electricity demand while the heat that it generates can be stored in the TST. This gives the system an additional flexibility that case 1 does not have.

Table 2
U Values of base case building used as input in the building information modelling software.

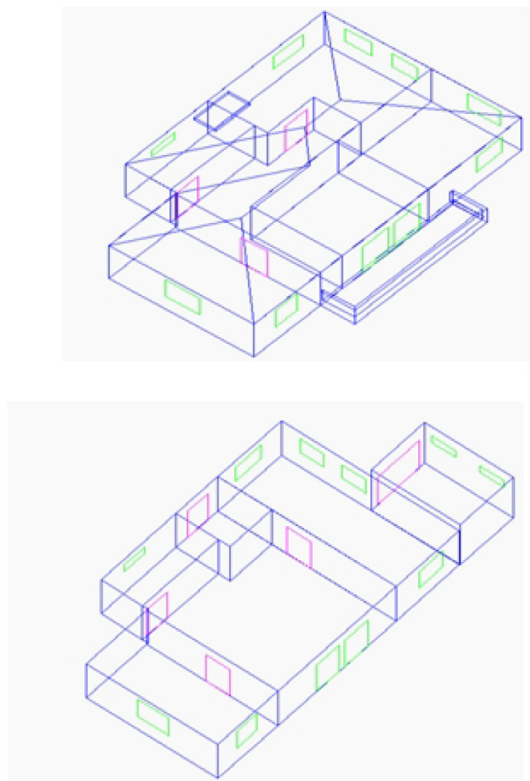|	U value (W/m² K)
Roof	0.20
Wall	0.30
Floor	0.25
Windows, Rooflights	2.00
Doors	2.00

Fig. 6. Image showing the structure of the 3D model and the two floors of the building. This image illustrates the process of creating the structure of the model by using series of rectangular blocks to develop the final shape of the building. The ground floor of the building is represented on the bottom image while the top floor and the roof on the top image.

5.2. Radiator system

Different heat emitters require different water temperatures and flow rates to efficiently deliver the heat output. In terms of modelling, the temperature bounds have been changed to allow for the higher temperatures of the radiator system. The fuel cell is assumed to operate at 80 °C to be able to supply an temperature of the same order at the cooling circuit. Similarly with cases 1 and 2, Cases 3 and 4 differ on the inclusion of TST in the design.

The higher pipe temperatures of the heating system are the characteristic in Case 3. This is best illustrated in Fig. 12 which zooms in again on the 288 dataset to show the pipe temperature leaving the fuel

cell cooling circuit and the afterburner heat exchanger for the first 48 h of the 288 data set. The resulting final supply and return pipe temperature at the heating and DHW circuits follow a 10 °C temperature difference while the flow rate varies to satisfy the demand.

The total water flow rates for case 3 follow the heat demand patterns as shown in Fig. 13. At times of no space heating demand, the flow rate takes the 0 value.

In Case 4 space heating and DHW demand are covered by all possible sources, the fuel cell cooling circuit, the afterburner, the gas boiler and the TST. A TST sized at 115 L provides heat to the system, reducing the operation of the gas boiler and allowing the fuel cell to cover most of the electricity demand minimising electricity import from grid. As the fuel cell is generating electricity in the summer when space heating demand is low, all heat is used for DHW.

The increased capacity of the fuel cell compared to cases 1 and 2 is a result of the more rapid space heating demand pattern of the radiator system. The average value of the hydrogen utilisation factor for the whole 288 h dataset is 0.63, which favours heat production compared to electricity. This is also supported by an average value for voltage of 0.64 V which is closer to the lower bounds of the variables and allows the fuel cell to produce more heat at both heat exchangers (and less electricity).

The total contribution of the TST in the whole heat demand combined is only 3%. This shows that for the case of a fuel cell sized to cover a big portion of space heating and DHW demand, the TST acts supportively ensuring that water is maintained at the high temperature at all times to be used when needed in the dwelling. The TST is not used as much as for the case of UFH system presented in case 2 because the higher temperature required for radiators is requires more heat to be achieved. The design in this case study has opted for a TST that is not used much. The design engineer looking at these results should make a decision with regard to the TST being required at all in the design.

In order to show the relation between the heat recovered from the fuel cell's cooling circuit and afterburner, to the water temperature in the pipe networks, Fig. 14 is used. At times of no heat output, e.g. between 144 h and 220 h, the supply stream temperature of the fuel cell heat exchanger takes a constant value of 50 °C; as the heating flow rate at these timesteps is 0, the temperature variables take the values that were used for initialisation.

5.3. Discussion

In terms of system sizing the optimum electrical capacity of the fuel cell is generally higher than most studies in literature and that can be considered an effect of the choice of the objective function. Hawkes et al. calculated an optimum fuel cell capacity between 0.9 kW and
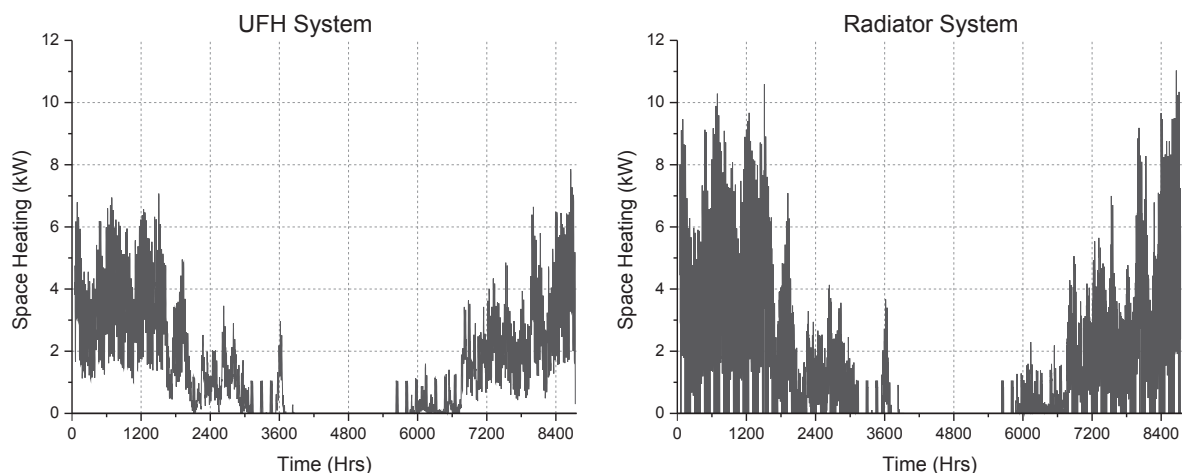

Fig. 7. Graph representing the annual energy demand for space heating of the base case for the two heating system options.
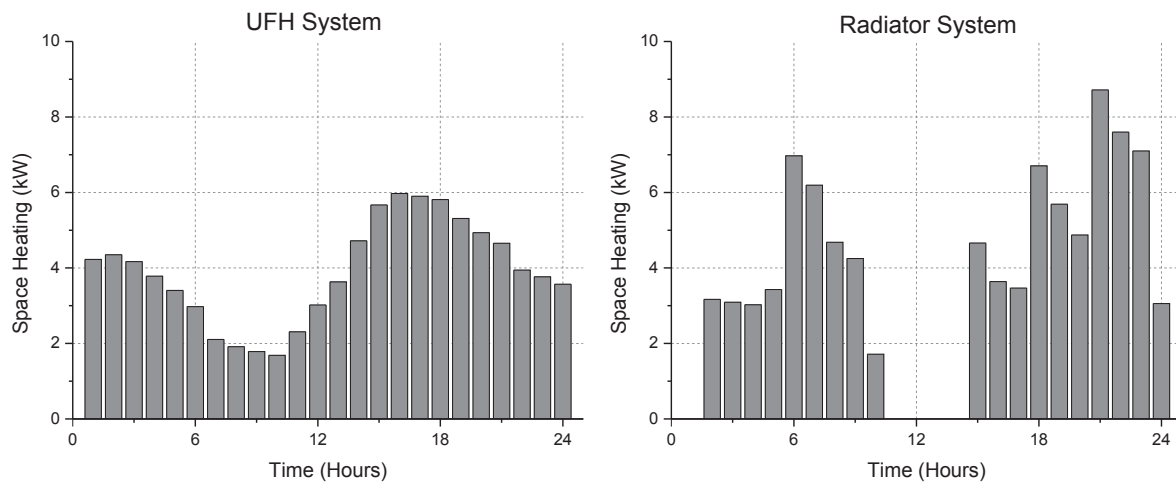
Fig. 8. Graph representing the winter space heating demand of the base case for the two heating system options on a 24-h segment of the complete annual dataset.

Table 3
Model statistics.

	Equations	Continuous variables	Discrete variables	CPU time (s)
Case 1	21,317	22,471	864	52
Case 2	21,320	22,759	576	3040
Case 3	21,317	22,471	864	53
Case 4	21,320	22,759	576	3043

Table 4
Summary of CO_2 emission results for all case studies.

	CO_2 emissions (kgCO_2)	Reduction (%)	Boiler CO_2 emissions (kgCO_2)	Fuel cell CO_2 emissions (kgCO_2)	Grid electricity CO_2 emissions (kgCO_2)
Base case	289	–	161	–	128
Case 1	211	27.0	60	135	16
Case 2	203	29.9	103	98	1
Base case	292	–	164	–	128
Case 3	209	28.4	82	125	2
Case 4	209	28.4	42	166	1

Table 5
Overview of system characteristics for all case studies. The results for case 4 stand out as higher capacity fuel cell is selected.

	Maximum boiler load heating (kW)	Maximum boiler load DHW (kW)	Maximum FC electrical capacity (kW)	TST volume (m³)
Base case	6.0	2.8	–	–
Case 1	5.6	1.0	1.9	–
Case 2	6	2.7	2.2	0.138
Base case	8.7	2.8	–	–
Case 3	6.2	1.5	1.9	–
Case 4	1.1	1.2	3.6	0.115

Table 6
Percentage annual heat contribution for space heating from all heat sources for all cases. Cases 1 and 3 that represent designs without thermal storage differ primarily on the amount of heat provided by the gas boiler while the results for Cases 2 and 4 suggest that for different heat emitters the operational schedule and overall design is changed.
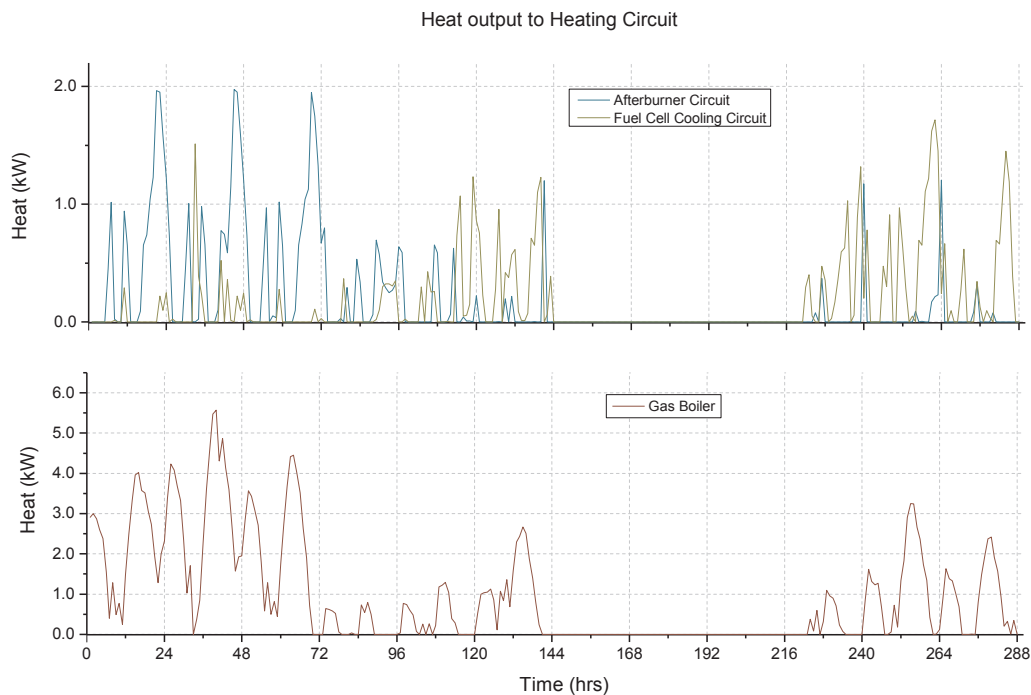
Source	Case 1 (%)		Case 2 (%)		Case 3 (%)		Case 4 (%)	
	Space heating	DHW	Space heating	DHW	Space heating	DHW	Space heating	DHW
FC cooling circuit	15	48	10	34	13	50	37	31
Afterburner	13	43	4	9	9	30	35	38
Gas boiler	72	9	82	54	78	20	27	29
TST	–	–	4	3	–	–	1	2

the majority of electricity (above 90% for all cases) covered by the fuel cell. The electrical led mode is easier to be followed by the fuel cell compared to the thermal because of its lower primary energy consumption. The thermal load profile is generally higher compared to the fuel cell capacity as also discussed by [33]. However case 4 which is a dwelling heated by radiators showed that a fuel cell sized higher compared to all other case studies can satisfy a big portion of the space heating demand. Generally for all configurations the fuel cell micro-CHP has the priority in operation and all the other systems around it run supportively. The UK Good Practice Guide 388 Combined heat and power for buildings suggests that regardless of the connection method, the CHP should operate as the lead boiler in order to maximise its operating hours. [34]. This is something shown in the results especially for the systems with TST which extend the fuel cell's operating hours.

Decisions on variable constraints and assumptions have been made to construct the model and these can affect the resulting designs.For instance, the upper bound of the fuel cell electrical capacity was set at 5 kW and although most products for domestic micro-generation applications are sized at smaller capacity, this allows the model to provide unconstrained results for this variable. This is true for case 4 where a higher capacity than most cases 3.6 kW fuel cell has been selected.

The comparison between the system design for slower heating systems such as UFH and for systems with radiators suggests that the fuel cell system can more easily handle the smooth demand pattern of the UFH system and covers a higher percentage of the demand. This is because of the ramp up rate constraints of the fuel cell.

Thermal storage increases predicted CO_2 savings compared to the cases without storage. Its inclusion in the design and the correct sizing reduces the use of gas boiler and grid electricity allowing the fuel cell to operate more hours. When the thermal and electrical demand profiles

1.3 kW by using cost as the objective function [32]. In terms of system operation and energy outputs, Napoli et al. performed both energy and economic analysis for fuel cell micro-CHP systems and found out that following the electrical demand profile is preferable in terms of energy and cost, as it increases the independence of the systems from the grid [33]. This is something that is demonstrated here as well as for most configurations examined, the fuel cell operation is electricity led with

Fig. 9. Graph representing how the system satisfies space heating demand utilising heat from the two fuel cell heat exchangers and the natural gas boiler for Case 1. No heat storage is considered in case 1.

follow different patterns, the additional heat produced by the fuel cell can be stored in a thermal storage tank. Storage tanks of larger volume are preferred for low temperature UFH systems while smaller tanks that be charged and achieve a higher 60–80 °C temperature are preferred for radiator systems. Barbieri et al. [35] makes a similar point concluding that the effect that the size of the thermal energy storage has on the system is not linearly correlated to the power of the fuel cell but is system specific. Bianchi et al. points out that energy performance of CHP units with an appropriately sized TST, can cover the overall

thermal energy demand of a dwelling providing savings in the order of 15–45%, depending on the CHP technology[36]. This is true for all case studies with more than 25% emissions reductions from the reference cases. In cases of high electricity demand covered by the fuel cell micro-CHP, there is surplus thermal energy which can be recovered in the TST. This generates the potential to increase the efficiency of the system as boiler use will be reduced.

The effect of climate has not fully been addressed in this study as the building modelled is located in London. However, in the case of a hot
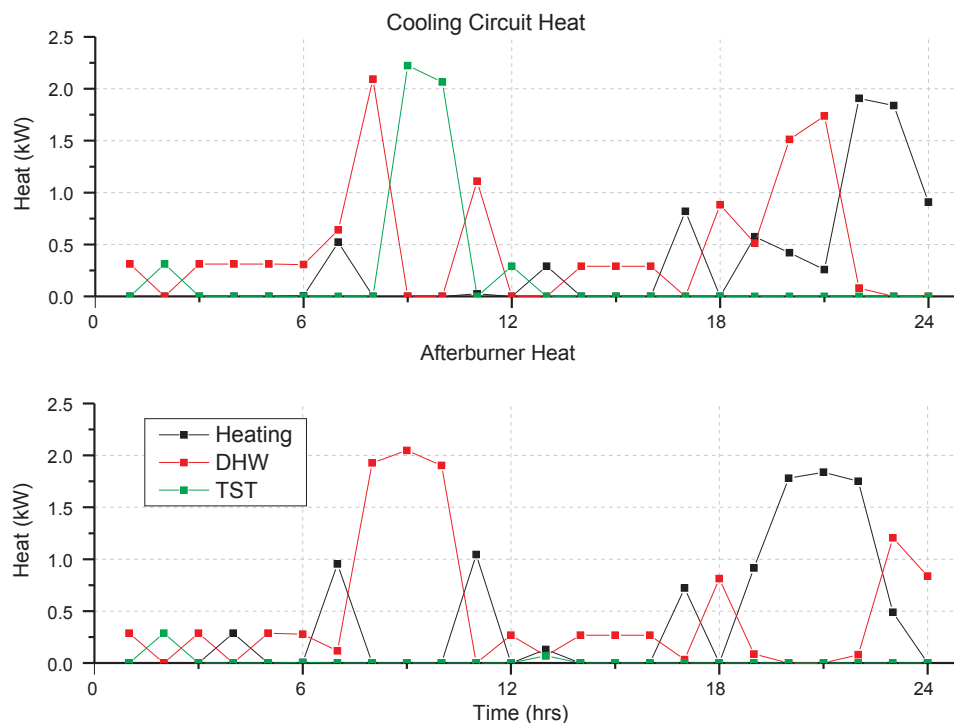
Fig. 10. Graph representing the heat extracted from the fuel cell and where this heat is delivered in the dwelling on a winter day for Case 2.
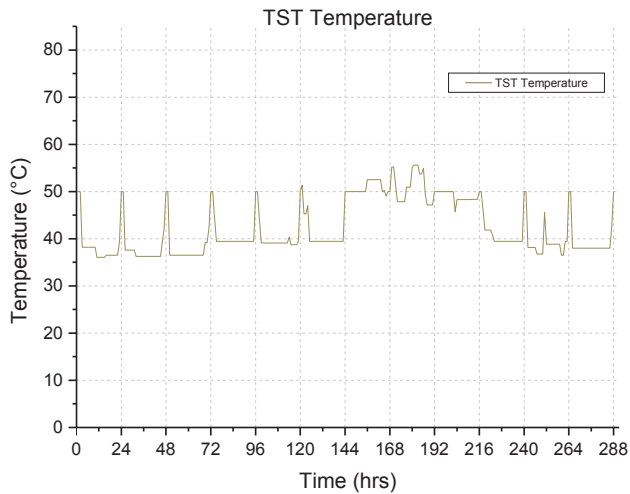
Fig. 11. Graph representing the variation of water temperature in the TST for Case 2. Case 2 allows the fuel cell micro-CHP, the gas boiler and TST to deliver heat to an UFH heating system.

summer with a high cooling demand (and a resulting high electricity demand), the expectancy is that the optimal fuel cell electrical capacity would increase to cover some of the demand, for the remaining to be covered by the electricity grid. The TST volume would also be increased to accommodate the additional heat. In cases of extreme winters, naturally we expect the boiler capacity to increase to cover the additional heating demand and heat from the TST to be utilised.

Barbieri [37], in a study that examined various micro-CHP technologies, concluded that the suitability of a micro-CHP technology in a dwelling increases when the power to heat ratio of the unit fits the power to heat ratio of the demand. This is the case here as the power to heat ratio of the fuel cell is better matched to the building under examination which is a high efficiency building. The influence of the

energy efficiency of the house on system performance has been studied by Gandiglio et al. [18]. In their study, in a high efficiency building, the PEMFC stack cogeneration heat can satisfy the thermal load required for the household. On the contrary PEMFC stacks for lower class buildings are able to provide only 20% of the required thermal power.

Stack degradation which occurs for a fuel cell at a rate of 1–$2\,\mu V\,h$ can increase with load cycling, start–stop cycles, low humidity at the stack, temperatures above 90 °C and lack of fuel in the anode [38]. In all cases presented here, the fuel cell operates at all times, generating the majority of electricity, so there are no start-stop cycles and no fuel starvation of the stack. The summer heat demand for DHW is the reason these problems are avoided as the fuel cell micro-CHP heat can be used for hot water generation.

The utilisation factor of hydrogen and voltage can act as a controlling measure of the fuel cell: when U^{fc} and voltage reduce, less electricity is produced at the fuel cell and more heat can be recovered from the afterburner as more hydrogen will be combusted. In the summer when less heat is required than the winter period, the utilisation factor takes values closer to its higher bound to maintain a high electricity output and to the reduce heat output.

An extra level of detail compared to other similar studies becomes available as the model's output contains the temperature and flow rates at the heat exchangers of the fuel cell micro-CHP system. This allows manufacturers and designers to size the micro-CHP heat exchangers. Also with the available information on temperature and flow rates, the heating and DHW network pipework can be sized and an approximation of the circulation pump's capacity can be obtained. This information will help building services designers choose the finalised pipework circuits. These circuits may include compensated heating circuits: The decision to include a three port valve in the heating circuit after the main heating header is something that can be determined because the exact variation of flow temperature is known.

The fuel cell stack temperature defines the cooling water temperature which will be used in the dwelling. In the few studies in literature that the heating system temperature constraints are taken into account,
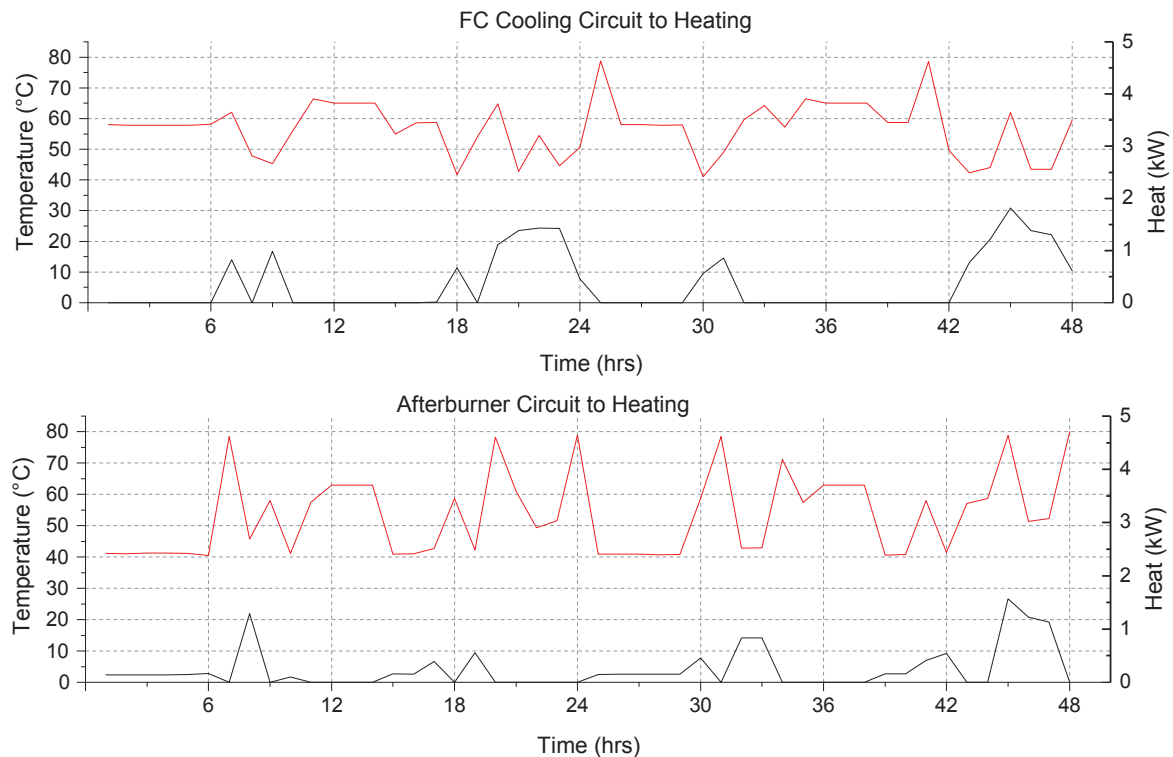

Fig. 12. Graph showing the supply temperatures of the fuel cell cooling circuit and afterburner heat exchangers over a period of 48 h for Case 3. Additionally the heat output of each heat exchanger to space heating is shown on the right axis.
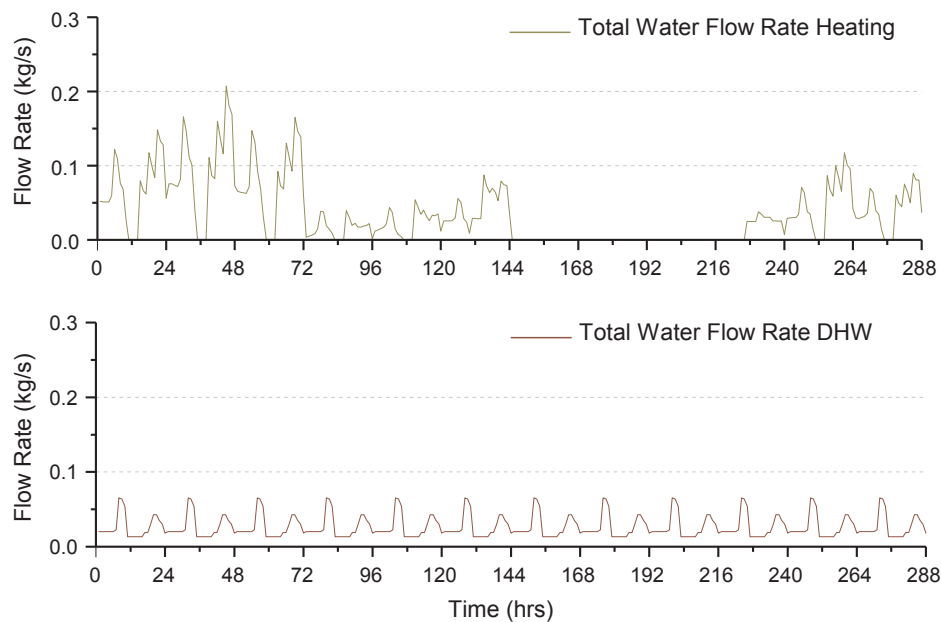
Fig. 13. Graph showing total water flow rates over the whole 288 h period for Case 3.
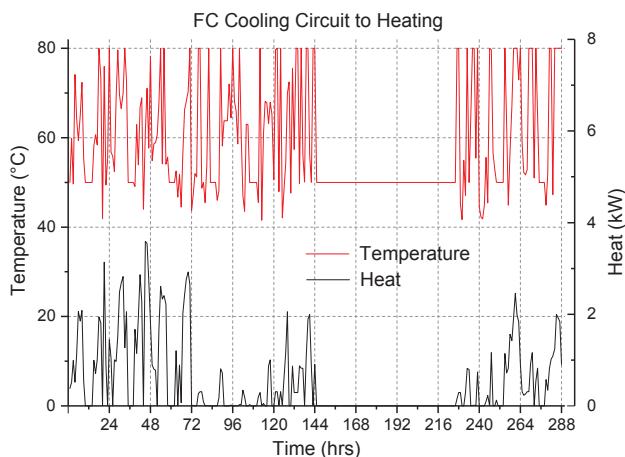

Fig. 14. Graph representing the supply temperature and heat released from the fuel cell cooling circuit to the space heating pipe circuit for Case 4.

the stack and exhaust temperatures are assumed to be constant at a certain level. Gandiglio et al. have assumed a stack temperature and afterburner exhaust of 62 °C and 120 °C respectively [18]. The model in this paper uses an optimisation framework and allows a varying temperature at the cooling and afterburner exhaust circuits obtained at the results. The varying flow rate and temperature at the heating and DHW circuits define the amount of heat that can be captured.

6. Conclusions

In this paper a MINLP model has been presented for optimising the design of a integrated system comprised of a PEMFC based micro-CHP and a dwelling's heating and DHW system. The proposed model, developed in GAMS, includes sub-models of the process units of the energy plant such as the fuel cell stack, reformer, afterburner, gas burner and also of the LTHW circuit that delivers heat to the building. The model identifies optimal ways of utilising available heat from the fuel cell's different heat exchangers at varying temperatures. A super-structure modelling approach has been developed which brings together modelling and optimisation with the specific attributes of the generating technology allowing for different grades of heat to be used

for different purposes. It designs the pipe network that delivers heat to the dwelling to satisfy heat demand calculating mass flow rates and pipe temperatures. It is a tool that can be used with little alterations in many case studies for many buildings and technologies. A series of case studies were developed to attempt to capture the effect of different heat emitting technologies on the design and operational conditions of the energy system of a dwelling. Also the presence of a thermal storage tank hasbeen evaluated. The results for confirm that a fuel cell micro-CHP system can reduce CO_2 emissions and satisfy household heat and electricity demand. The predicted emissions reduction compared to the base case reference building which was developed using building modelling software vary from 27% to approximately 30%. Modelling the flow and temperatures in the heat exchangers allows a design based on the selected heating system. The correct design of the fuel cell thermal management system ensures that heat from the fuel cell stack and the fuel processing system can be used effectively. The amount of heat delivered by the fuel cell cooling circuit and afterburner combined range between 16–72% and 43–91% for heating and DHW respectively. For all cases the fuel cell micro-CHP is delivering the majority of the dwelling's electricity demand minimising the need for grid electricity.

However, the fact that the temporal precision of the model is in hourly timesteps does not allow the minute by minute variability of power and heat demand to be captured. Therefore the results carry the assumption of a constant load within this hourly timestep. The peaks in energy demand that occur usually for a short amount of time are averaged in the 1-h period. A model based on a 5-min timestep run for a few hours could capture the variations in electricity and heat demand that occur in this shorter period. The fuel cell micro-CHP and all plant would have to respond to these demands and that could uncover their limitations in terms of ramping up or down. In timesteps that e.g. a 50% increase in the electricity demand occurs that cannot be satisfied by the fuel cell, grid electricity will be used. This element cannot be captured by models using hourly timesteps. Despite this limitation, the benefit of a yearly dataset is that it can capture the seasonal variation of all demands and deliver a design that can satisfy them.

Future work will focus on expanding this optimisation framework to consider additional technologies that can be used in buildings. Hybrid systems such as a fuel micro-CHP coupled with ground source heat pumps can be modelled. Different prime movers such as Stirling engines and internal combustion engines can be added to drive the micro-CHP. As each one of them have different heat to power ratios, the resulting

design would be interesting to evaluate.

Acknowledgements

References

[1] International Energy Outlook 2017, U.S. Energy information administration; 2017.

[2] Digest of United Kingdom Energy Statistics 2011. Department of energy and climate change; 2011.

[3] Hawkes A, Brett DJL, Brandon NP. Fuel cell micro-CHP techno-economics: part 1 model concept and formulation. Int J Hydrogen Energy 2009;34:9545–57. http://dx.doi.org/10.1016/j.ijhydene.2009.09.094. ISSN 0360-3199.

[4] Ang SMC, Fraga ES, Brandon NP, Samsatli NJ, Brett DJL. Fuel cell systems optimisation methods and strategies. Int J Hydrogen Energy 2011;36:14678–703. http://dx.doi.org/10.1016/j.ijhydene.2011.08.053. ISSN 0360-3199.

[5] Staffell I, Green R, Kendall K. Cost targets for domestic fuel cell CHP. J Power Sour 2008;181:339–49. http://dx.doi.org/10.1016/j.jpowsour.2007.11.068. ISSN 0378-7753.

[6] Tapia-Ahumada K, PTrez-Arriaga I, Moniz E. A methodology for understanding the impacts of large-scale penetration of micro-combined heat and power. Energy Policy 2013;61:496–512. http://dx.doi.org/10.1016/j.enpol.2013.06.010. ISSN 0301-4215.

[7] Dodds P, Staffell I, Hawkes A, Li F, Grnnewald P, McDowall W, et al. Hydrogen and fuel cell technologies for heating: a review. Int J Hydrogen Energy 2015;40(5):2065–83. http://dx.doi.org/10.1016/j.ijhydene.2014.11.059. ISSN 0360-3199.

[8] Hawkes AD, Aguiar P, Hernandez-Aramburo CA, Leach MA, Brandon NP, Green TC, et al. Techno-economic modelling of a solid oxide fuel cell stack for micro combined heat and power. J Power Sour 2006;156:321–33. http://dx.doi.org/10.1016/j.jpowsour.2005.05.076. ISSN 0378-7753.

[9] Hawkes AD, Brett DJL, Brandon NP. Fuel cell micro-CHP techno-economics: part 2 model application to consider the economic and environmental impact of stack degradation. Int J Hydrogen Energy 2009;34:9558–69. http://dx.doi.org/10.1016/j.ijhydene.2009.09.095. ISSN 0360-3199.

[10] Arsalis A, Nielsen MP, Kaer SK. Modeling and off-design performance of a 1 kWe HT-PEMFC-based residential micro-CHP system for Danish single-family households. J Energy 2011;36:993–1002. http://dx.doi.org/10.1016/j.energy.2010.12.009. ISSN 0360-5442.

[11] Arsalis A, Nielsen MP, Kaer SK. Modeling and parametric study of a 1 kWe HT-PEMFC-based residential micro-CHP system. Int J Hydrogen Energy 2011;36:5010–20. http://dx.doi.org/10.1016/j.ijhydene.2011.01.121. ISSN 0360-3199.

[12] Ashari GR, Ehyaei MA, Mozafari A, Atabi F, Hajidavalloo E, Shalbaf S. Exergy, economic, and environmental analysis of a PEM fuel cell power system to meet electrical and thermal energy needs of residential buildings. J Fuel Cell Sci Technol 9. ISSN 1550-624X.

[13] Barelli L, Bidini G, Gallorini F, Ottaviano A. Dynamic analysis of PEMFC-based CHP systems for domestic application. J Appl Energy 2012;91:13–28.

[14] Dorer V, Weber R, Weber A. Performance assessment of fuel cell micro-cogeneration systems for residential buildings. Energy Build 2005;37:1132–1146, ISSN 0378-778. http://dx.doi.org/10.1016/j.enbuild.2005.06.016.

[15] Gigliucci G, Petruzzi L, Cerelli E, Garzisi A, Mendola AL. Demonstration of a residential CHP system based on PEM fuel cells. J Power Sour 2004;131(1–2):62–8. http://dx.doi.org/10.1016/j.jpowsour.2004.01.010. ISSN 0378-7753.

[16] Ang SMC, Brett DJL, Fraga ES. A model for the multi-objective optimisation of a polymer electrolyte fuel cell micro-combined heat and power system. Comp Aided Chem Eng 2010;28(C):949–54. http://dx.doi.org/10.1016/S1570-7946(10)28159-2.

[17] Mago PJ, Luck R. Evaluation of the potential use of a combined micro-turbine organic Rankine cycle for different geographic locations. Appl Energy 2013;102(0):1324–33. http://dx.doi.org/10.1016/j.apenergy.2012.07.002 ISSN 0306-2619, special Issue on Advances in sustainable biofuel production and use - International Symposium on Alcohol Fuels.

[18] Gandiglio M, Lanzini A, Santarelli M, Leone P. Design and optimization of a proton exchange membrane fuel cell CHP system for residential use. Energy Build 2014;69:381–93. http://dx.doi.org/10.1016/j.enbuild.2013.11.022. ISSN 0378-7788.

[19] Barbieri ES, Melino F, Morini M. Influence of the thermal energy storage on the profitability of micro-CHP systems for residential building applications. J Appl Energy 2012;97:714–22. http://dx.doi.org/10.1016/j.apenergy.2012.01.001. ISSN 0306-2619.

[20] Bianchi M, Pascale AD, Melino F. Performance analysis of an integrated CHP system with thermal and electric energy storage for residential application. Appl Energy 2013;112(0):928–38. http://dx.doi.org/10.1016/j.apenergy.2013.01.088. ISSN 0306-2619.

[21] Shaneb OA, Taylor PC. An evaluation of integrated fuel cell and energy storage systems for residential applications. In: Upec:2009 44th international universities power engineering conference, ISBN 978-1-4244-6823-2; 2009.

[22] Adam A, Fraga ES, Brett DJL. Options for residential building services design using fuel cell based micro-CHP and the potential for heat integration. Appl Energy 2015;138:685–94. http://dx.doi.org/10.1016/j.apenergy.2014.11.005. ISSN 0306-2619.

[23] Fuel Cell Handbook. U.S. Department of Energy Office of Fossil Energy National Energy Technology Laboratory, 7th ed. EG&G Technical Services, Inc.; 2004.

[24] Hoogers G, editor. Fuel cell technology handbook. CRS Press; 2003.

[25] Woo CH, Benziger JB. PEM fuel cell current regulation by fuel feed control. Chem Eng Sci 2007;62(4):957–68. http://dx.doi.org/10.1016/j.ces.2006.10.027. ISSN 0009-2509.

[26] Larminie J, Dicks A. Fuel cell systems explained. 2nd ed. Wiley; 2003.

[27] Government GHG Conversion Factors for Company Reporting: Methodology Paper for Emission Factors, Department of Environment, Food and Rural Affairs; 2013 < https://goo.gl/bj5Evg > .

[28] The Building Regulations 2010. Conservation of fuel and power in new dwellings, Approved Document 2013 Edition. HM Government; 2013.

[29] Domestic building services compliance guide 2010 Edition. HM Government, ISBN 9781859463772; 2010.

[30] Brooke A, Kendrick D, Meeraus A, Raman R. GAMS - a user's guide. GAMS Development Corporation; 2008 < https://www.gams.com/ > .

[31] Misener R, Floudas CA. ANTIGONE: Algorithms for coNTinuous/Integer Global Optimization of Nonlinear Equations. J Global Optim 2014;59(2):503–26. http://dx.doi.org/10.1007/s10898-014-0166-2. ISSN 1573-2916.

[32] Hawkes AD, Aguiar P, Croxford B, Leach MA, Adjiman CS, Brandon NP. Solid oxide fuel cell micro combined heat and power system operating strategy: options for provision of residential space and water heating. J Power Sour 2007;164:260–71. http://dx.doi.org/10.1016/j.jpowsour.2006.10.083. ISSN 0378-7753.

[33] Napoli R, Gandiglio M, Lanzini A, Santarelli M. Techno-economic analysis of PEMFC and SOFC micro-CHP fuel cell systems for the residential sector. Energy Build 2015;103:131–46. http://dx.doi.org/10.1016/j.enbuild.2015.06.052. ISSN 0378-7788.

[34] UK Good Practice Guide GPG 388: Combined heat and power for buildings. Action energy; 2004 < https://goo.gl/nQh53X > .

[35] Barbieri ES, Melino F, Morini M. Influence of the thermal energy storage on the profitability of micro-CHP systems for residential building applications. Appl Energy 2012;97(0):714–22. http://dx.doi.org/10.1016/j.apenergy.2012.01.001. ISSN 0306-2619.

[36] Bianchi M, De Pascale A, Spina P. Guidelines for residential micro-CHP systems design. J Appl Energy 2012;97:673–85. http://dx.doi.org/10.1016/j.apenergy.2011.11.023. ISSN 0306-2619.

[37] Barbieri E, Spina P, Venturini M. Analysis of innovative micro-CHP systems to meet household energy demands. J Appl Energy 2012;97:723–33. http://dx.doi.org/10.1016/j.apenergy.2011.11.081. ISSN 0306-2619.

[38] de Bruijn FA, Dam VAT, Janssen GJM. Review: durability and degradation issues of PEM fuel cell components. Fuel Cells 2008;8(1):3–22. http://dx.doi.org/10.1002/fuce.200700053. ISSN 1615-6854.